

## Research article

Viktoriia E. Babicheva\* and Jerome V. Moloney

# Lattice effect influence on the electric and magnetic dipole resonance overlap in a disk array

<https://doi.org/10.1515/nanoph-2018-0107>

Received July 26, 2018; revised August 19, 2018; accepted August 30, 2018

**Abstract:** Designing the shape of silicon nanoparticles has been shown to be an effective approach to increasing overlap between electric and magnetic dipole resonances thereby achieving directional scattering and decrease of reflection. Variations of disk diameter and/or height affect resonances differently and can thus result in resonance overlap. In most of the studies, the disks are arranged in a periodic array where the periodicity is varied together with disk diameter, but the role of lattice effect is neglected. Here we theoretically study a periodic array of disks and show that the contribution of the lattice effect in shifting resonance positions is comparable to the effect of the diameter change. We demonstrate that the lattice effect is important even when the wavelength of diffraction remains on the blue side from electric and magnetic dipole resonances and there are no additional lattice resonances excited. Period and disk dimensions are chosen so that the resonances overlap in the proximity of the telecommunication wavelength which is of great practical interest.

**Keywords:** collective resonance; directional scattering; Kerker effect; nanoparticle array; silicon particles.

Subwavelength nanostructures have been actively studied with the aim of being applied in optical and photonic devices, for sensing [1], photovoltaics [2, 3], optical communications [4], detectors [5], functional elements, including metasurfaces [6], directional scattering and enhanced light-matter interaction [7], high-resolution near-field microscopy [8], and others. Various nanoparticle shapes [9, 10] and materials [11, 12] have been proposed to serve

as building blocks to enhance resonances and increase scattering and/or absorption. Recently, high-index dielectrics, such as silicon, germanium, and III–V compounds, have been shown to be a promising platform for realizing subwavelength nanoantennas. The operation bandwidth of such nanostructures is mainly defined by the material optical properties and particle dimensions. Larger or smaller particles can shift resonances to larger or smaller wavelength, correspondently. Thus, with the silicon particles, the effect can be achieved in the mid-infrared or visible spectral range. However, material losses may hinder nanostructure performance, and in general, it is desirable to operate at the energies below the semiconductor bandgap (e.g. 1.1 eV = 1.13  $\mu\text{m}$  for silicon).

One of the advantages of high-index antennas over conventional plasmonic particles is the possibility of exciting both electric and magnetic resonances in particles of simple shape, such as spheres or disks [13, 14]. The strong electric and magnetic resonance excitations and their interference in high-index nanostructures open a unique opportunity for designing optical nanoantennas and metasurfaces with a considerable enhancement of the nonlinear response [15]. While silicon possesses an almost negligible second-order nonlinearity of bulk material, other semiconductors such as aluminum gallium arsenides can bring a significant enhancement. It drives a rapid progress in developing nonlinear optical nanostructures beyond the diffraction limit and useful applications in nonlinear photonic metadevices operating at the nanoscale [16, 17]. A dynamic control of optical response of semiconductor nanoparticle arrays can be achieved either by combining them with elements of other materials with the strong dynamic response, such as vanadium dioxide [18] or ferroelectrics [19], or by inducing a switch in the semiconductor itself. For example, semiconductor nanoparticles, including silicon and III–V compounds, designed as nonlinear resonators can be utilized for ultrafast switching [20]. The transient modulation of the material permittivity by variations of electron-hole plasma density induced via its photoexcitation by a femtosecond laser has been shown to significantly alter the scattering behavior of silicon nanoparticles [21].

\*Corresponding author: **Viktoriia E. Babicheva**, College of Optical Sciences, University of Arizona, 1630 E. University Blvd., PO Box 210094, Tucson, AZ 85721, USA, e-mail: vb2@email.arizona.edu. <http://orcid.org/0000-0002-0789-5738>

**Jerome V. Moloney:** College of Optical Sciences, University of Arizona, PO Box 210094, Tucson, AZ 85721, USA

The interplay of resonances, for instance, their overlap, offers the potential to tune scattering and engineer more efficient subwavelength antennas. The Kerker effect is defined as near-zero backward scattering when electric (ED) and magnetic dipole (MD) moments of the particle are equal in magnitude and in phase [22–24]. In a similar way, one can achieve a strong backward reflection in the structure where ED and MD moments are out of phase. One can utilize such nanoparticle array to compensate reflection from the high-index substrate, and in this case, the array serves as an antireflective coating [2, 25].

One of the practical interests is to achieve the Kerker effect when multipole moments are in resonant states, and for instance, ED and MD resonances overlap (EDR and MDR, respectively). For silicon spherical particles this is not possible, but adjustment of diameter and/or height of disk particles or designing particle shape can bring resonances into overlap [10, 26]. The effect of disk height with fixed diameter has been studied for a single silicon particle in detail proving the EDR and MDR shift differently upon height changes [26]. The seminal work [6] demonstrates the EDR and MDR overlap in the array of disks, and this overlap is attributed to the changes in the disk diameter. However, together with the disk dimensions,

the distance between disks in the array is also varied, and the effect of these changes has remained overlooked in [6]. As we show in the present work, nanoparticle resonances are strongly affected by their arrangement even in the case of subdiffraction distances, and this effect can play a crucial role in defining the resonance positions and their overlap.

Arranging particles in an array adds new features to the spectrum of optical response as the contribution of all particles in the lattice affects the resonance position. Rectangular lattices, where the particles are periodic and equally spaced in mutually perpendicular directions (e.g. periods  $D_x$  and  $D_y$  in the  $x$ - and  $y$ -directions, Figure 1A), have been studied in detail. The best known and studied effect is lattice resonance [1, 3, 11, 27–35], which is an additional narrow resonance in the proximity to the wavelength of diffraction, the so-called Rayleigh anomaly. Usually, the most pronounced lattice resonance is excited when the Rayleigh anomaly is on the red side from the single-particle resonance. It has been shown that the lattice resonance can be an excitation of the ED or MD [11] as well as electric quadrupole [31, 34], and by analogy, one can expect that higher multipoles can also contribute to the lattice resonance [36].

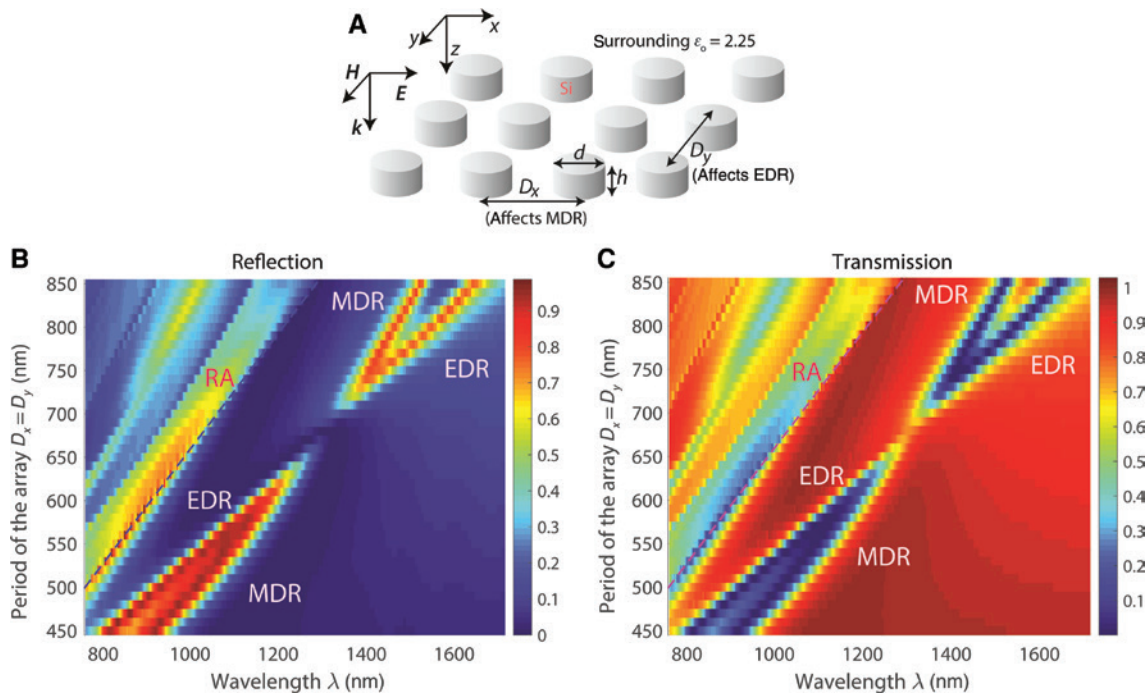


**Figure 1:** Overlap of electric and magnetic dipole resonances in the square disk array.

(A) Schematics of the structure under consideration: periodic array of disks and normal incidence of the light with the E field along the  $x$ -axis. The surrounding medium has  $\epsilon_0 = 2.25$ . For this polarization, the array period in the  $x$ -direction  $D_x$  affects excitation of a magnetic dipole resonance (MDR), and the period in the  $y$ -direction  $D_y$  affects the electric dipole resonance (EDR). (B) Reflection and (C) transmission through the disk array under variation of the array periods and disk diameters with  $D_x = D_y = d + 200$  nm. The dashed blue and red lines mark the Rayleigh anomaly wavelength  $\lambda_{RA} = D_x = D_y$ .

In the present work, we consider only dipole moments of the disk particle as higher multipole contributions in the scattering properties of the silicon disk with such dimensions are negligible in comparison to dipole contributions (see calculations of the different multipole moments for the similar size disk in [37]). For a dipole array, the lattice effect is defined by the periodicity in the direction of dipole emission. It has been shown previously that when an electric field of the incident plane wave is polarized along the  $x$ -axis, the array period in the  $D_x$  direction affects the MD moment and is responsible for the excitation of an additional MD lattice resonance [11]. Correspondingly, in the same polarization, tuning the period  $D_y$  affects the ED moment and is responsible for an ED lattice resonance (Figure 1A). Thus, ED and MD lattice resonances can be independently controlled by varying the mutually perpendicular array periods, and the lattice resonances can be brought into overlap without imposing limitations on particle shape [33, 38].

As the lattice resonance is typically narrow and appears as an additional resonance in the proximity to the Rayleigh anomaly wavelength, the lattice resonance is usually easy to recognize. However, much less attention has been paid to another signature of the lattice effect, such as a change of resonance profile and spectral position when the Rayleigh anomaly is on the blue side from the single-particle resonance and no additional lattice resonance is excited. Furthermore, there is a misconception that the lattice effect can be neglected once the single-particle resonance is on the red side from Rayleigh anomaly [6, 37, 39]. This assumption is not valid, and here we show that taking into account array periodicity is important even if particle resonances are spectrally separated from Rayleigh anomaly and the latter one is on a blue side from the resonance.

In the present work, we report on the theoretical observation of the lattice effect in a disk array, and we directly compare the lattice effect on the EDR and MDR shifts to the adjustment of disk diameter. We demonstrate that the array period and disk diameter have a comparable contribution to the resonance positions. We choose array parameters the same as in the experimental work [6], and EDR and MDR overlap in the proximity of the telecommunication wavelength. We show that the EDR and MDR overlap should be attributed to not only change of particle shape but also to the array periodicity.

We study a periodic array of disks with permittivity  $\varepsilon = 12.25 + 0.05i$  (silicon), diameter  $d$ , fixed height  $h = 220$  nm, arranged in the array with periods  $D_x$  and  $D_y$ , and surrounded by a medium with fixed permittivity  $\varepsilon_0 = 2.25$  (Figure 1A). Disk shape has a particular advantage

from the practical point of view: in contrast to elliptical particles, it can be straightforwardly fabricated with lithographical methods, and in contrast to cuboids, disks do not have sharp edges in an in-plane direction that require additional precision in fabrication. The disk array can be fabricated by structuring a silicon layer on a fused silica substrate via an electron-beam lithography-based process (for similar arrays, the details of structure fabrication and characterization can be found in [6, 37, 39]). We perform numerical simulations with the finite-difference time-domain method with an in-house package. The unit cell contains one disk, periodic boundary conditions in the  $x$ - and  $y$ -directions, and perfectly matched layers in the  $z$ -direction, and light is incident normal to the array with the E field along the  $x$ -axis.

To start with, we perform a study similar to the one in [6]: we vary simultaneously  $d$ ,  $D_x$ , and  $D_y$  satisfying the condition  $D_x = D_y = d + 200$  nm and calculate reflection from the array (Figure 1B). In agreement with results for the disk array in [6], we see that under the condition  $d = 500$  nm, EDR and MDR spectrally overlap and reflection is suppressed to a near-zero value. Transmission calculations complement the reflection map and confirm resonance overlap and increased transmission for  $d = 500$  nm (Figure 1C).

One can compare particle resonances in the array to the single particle resonances. In our case, resonances of the single silicon disk (without the array) with the same height but varying diameter are calculated in [6] and indicate that EDR and MDR overlap occurs for  $d = 290$  nm at the wavelength of about 1050 nm. The calculations also show that for the single disk with  $d = 500$  nm, MDR and EDR positions are  $\lambda_{\text{MDR}} \approx 1350$  nm and  $\lambda_{\text{EDR}} \approx 1600$  nm, respectively. Obviously, the optimum disk diameter and wavelength of the resonances calculated for a single disk are very different from the parameters calculated for the disk array, in both [6] and the present work (Figure 1B and C). This discrepancy is caused by the lattice effect of compactly arranged particles in the array, and the lattice contribution cannot be neglected in this case.

As the arrangement of particles in the array plays a crucial role in the position of particle resonances, let us consider what structural parameters affect the disk resonances. Resonance overlap and reflection suppression in Figure 1 are a typical manifestation of the Kerker effect; however, the simultaneous changes of  $d$ ,  $D_x$ , and  $D_y$  cause an ambiguity in identifying the main cause of EDR and MDR spectral shifts. The work [6] ascribes the effect of resonance overlap solely to the changes in disk diameter. The changes of EDR and MDR positions are described as if they were excited in a single particle. However, along with the

diameter change, the array periods change as well, and below we show that this period variation strongly affects the resonance position.

Let us analyze what effect causes changes in the array period rather than the effect of disk diameter. Figure 2A shows calculations for  $D_y=700$  nm,  $d=500$  nm, and different  $D_x$ . One can see that the position of EDR is fixed to  $\lambda \approx 1350$  nm and MDR changes the position from  $\lambda_{550} \approx 1180$  nm to  $\lambda_{850} \approx 1450$  nm remaining parallel to the Rayleigh anomaly. Similar to Figure 1B, the resonance overlap causes a reflection suppression which means that the conditions for the Kerker effect are satisfied. As the resonance position is defined by the lattice period, either EDR or MDR can be excited at a larger wavelength (either  $\lambda_{\text{MDR}} > \lambda_{\text{EDR}}$  or  $\lambda_{\text{MDR}} < \lambda_{\text{EDR}}$ ) depending on the particular period values, so the order of resonances in Figure 2A is different from the one in Figure 1B. Both EDR and MDR maintain a spectral separation  $\Delta\lambda = \lambda_{\text{EDR(MDR)}} - \lambda_{\text{RA-EDR(MDR)}} \approx 200$  nm from the position of Rayleigh anomaly that they correspond to  $\lambda_{\text{RA-EDR}} = D_y = 700$  nm and  $\lambda_{\text{RA-MDR}} = D_x$ . In Figure 2A, we see that at the large  $D_x$ , the MDR is closer to Rayleigh anomaly than for the small  $D_x$ , and it is a general property of the lattice effect in the nanoparticle array: the sparser the array the closer the resonance to Rayleigh anomaly wavelength. Similar to the effect of  $D_x$  changes and MDR shift, the orthogonal period  $D_y$  variation causes an EDR shift (Figure 2B). In both panels of Figure 2, the disk diameter is fixed to  $d=500$  nm, and the calculation results indicate that resonance position

is strongly affected by the changes of array period even for the fixed disk size. The results in Figure 1 and work [6] cannot be ascribed solely to the effect of diameter change and need to account for the array periodicity.

Finally, let us consider separate changes of lattice period and disk diameter in the structure that follow the initial case of geometry with  $D_x = D_y = d + 200$  nm. To differentiate the effects of lattice and disk diameter changes and compare contributions from each of them on the resonance position, we separately change  $D_x$ ,  $D_y$ , and  $d$  and analyze changes in reflection profiles (Figure 3). We choose two sets  $D_x = 450$  nm and  $D_x = 500$  nm, and both sets satisfy the initial condition  $D_x = D_y = d + 200$  nm. For the intermediate step  $D_x = 500$  nm,  $D_y = 450$  nm, and  $d = 250$  nm, we see that the MDR shift due to the change in  $D_x$  from 450 to 500 nm (black to cyan line) is comparable to the effect of the change in  $d$  from 250 to 300 nm (cyan to blue line, Figure 3A). Similarly, for the intermediate step  $D_x = 450$  nm,  $D_y = 500$  nm, and  $d = 250$  nm, the calculations show that the EDR shift due to the change in  $D_y$  from 450 to 500 nm (black to red line) is comparable to the effect of the change in  $d$  from 250 to 300 nm (red to blue line, Figure 3B). Figure 3 shows calculations only for two sets of parameters, but the conclusion is valid for larger periods and disk diameters, and the lattice effect should be taken into account in such particle arrays.

To sum up, we have considered a silicon particle array which is optimized to increase transmission and resonantly scatter light in the forward direction in the telecommunications wavelength range. In particular, the reflection from

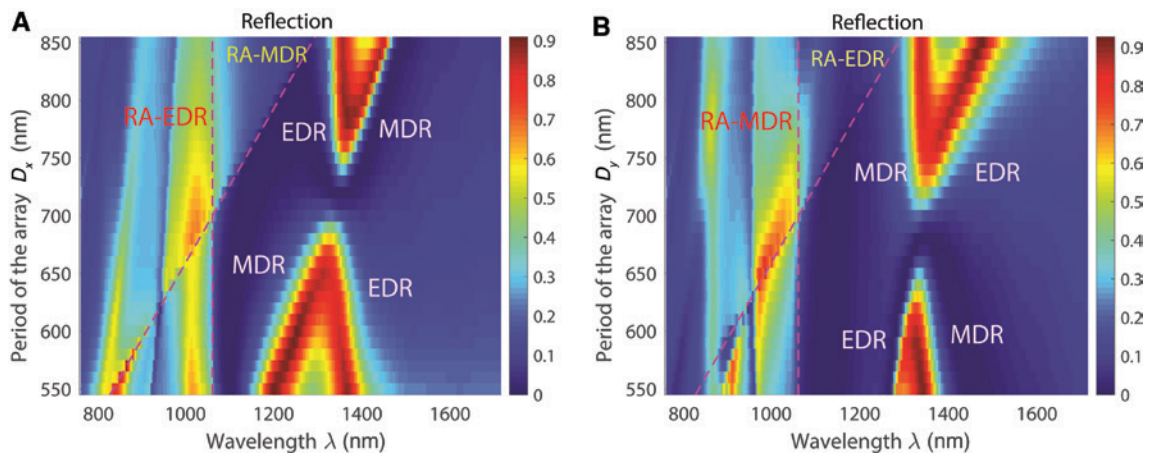


**Figure 2:** Reflection of the disk array under independent variations of (A)  $D_x$  and (B)  $D_y$ . The second period is fixed at 700 nm, and the diameter  $d=500$  nm is fixed and the same on both panels. In (A), changes in  $D_x$  cause magnetic dipole resonance (MDR) shift, but  $D_y$  and electric dipole resonance (EDR) position remain unchanged. In (B),  $D_y$  changes cause the EDR shift, but  $D_x$  and MDR position remain unchanged. The dashed magenta lines mark the Rayleigh anomaly wavelength:  $\lambda_{\text{RA-EDR}} = D_y = 700$  nm and  $\lambda_{\text{RA-MDR}} = D_x$  in (A), and  $\lambda_{\text{RA-MDR}} = D_x = 700$  nm and  $\lambda_{\text{RA-EDR}} = D_y$  in (B). Both EDR and MDR remain on spectral distance about  $\Delta\lambda \approx 200\text{--}350$  nm from the corresponding Rayleigh anomaly wavelength.

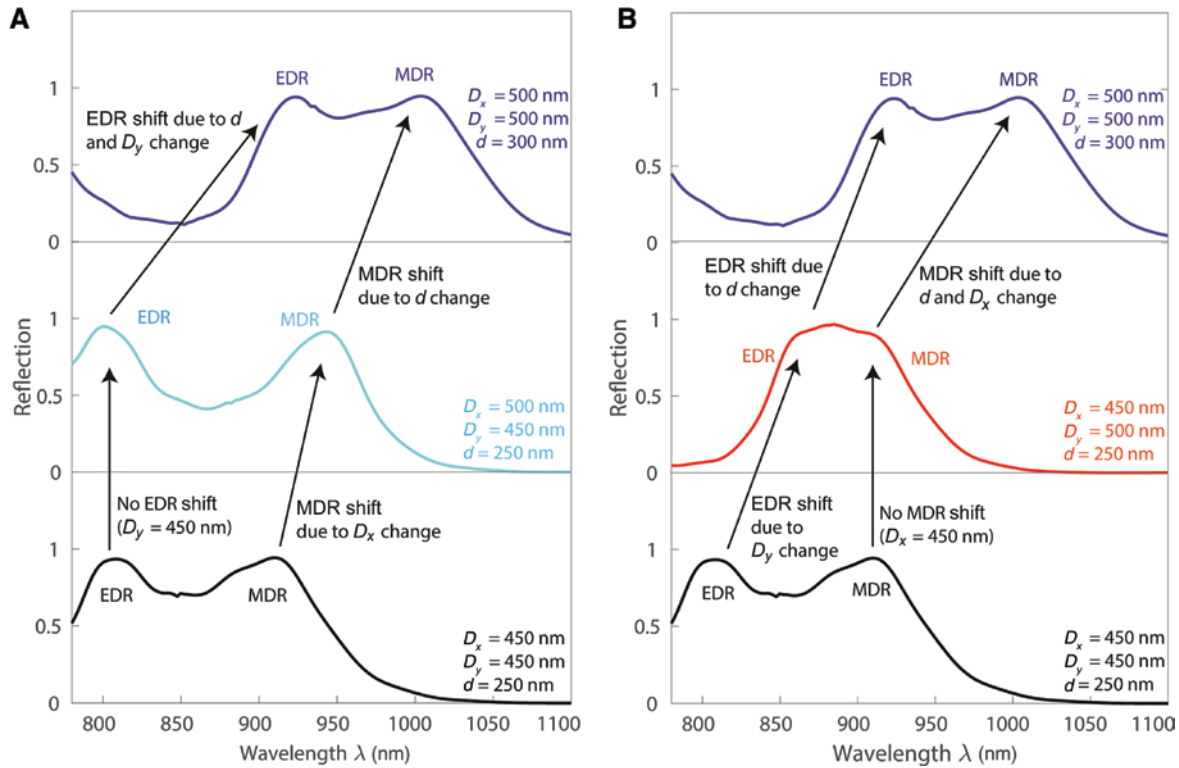


**Figure 3:** Contrast of lattice and disk diameter variation influence: consequent changes of  $D_x$ ,  $D_y$ , and  $d$  between the cases

$D_x = D_y = d + 200 \text{ nm} = 450 \text{ nm}$  and  $D_x = D_y = d + 200 \text{ nm} = 500 \text{ nm}$ .

(A) The intermediate step is  $D_x = 500 \text{ nm}$ ,  $D_y = 450 \text{ nm}$ , and  $d = 250 \text{ nm}$ , and the magnetic dipole resonance (MDR) shift caused by the change in  $D_x$  (black to cyan line) is comparable to the effect of the change in  $d$  (cyan to blue line). (B) The intermediate step is  $D_x = 450 \text{ nm}$ ,  $D_y = 500 \text{ nm}$ , and  $d = 250 \text{ nm}$ , and the electric dipole resonance (EDR) shift caused by the change in  $D_y$  (black to red line) is comparable to the effect of the change in  $d$  (red to blue line).

the array is nearly zero and transmission is almost 100% at the wavelength 1300 nm, which is achieved for the array with silicon disk particles 470 nm in diameter and 220 nm in height arranged into the square array with the period of 670 nm. We have studied a periodic array of disks with various dimensions and analyzed the effect of lattice period and disk diameter on the EDR and MDR position and their overlap. We have shown that resonance position can be changed by the period, and EDR and MDR can be brought into overlap solely by the change of array period having disk diameter fixed. We emphasize that the Rayleigh anomaly remains on the blue side from the resonance and no additional resonances (so-called lattice resonances) are excited in the structure. The lattice effect plays a crucial role in this structure, and EDR and MDR closely follow the corresponding Rayleigh anomaly and mainly defined by its position even though the resonances are about  $\Delta\lambda \approx 200\text{--}350 \text{ nm}$  away from Rayleigh anomaly. We have also shown that the lattice effect is comparable to the effect of disk size change, and thus cannot be neglected in the closely spaced particle arrays despite the resonances excited at the wavelength larger than Rayleigh anomaly.

**Acknowledgments:** The authors thank John Nehls and Colm Dineen for the help with the cluster machine. This material is based upon work supported by the Air Force Office of Scientific Research, Funder Id: <http://dx.doi.org/10.13039/100000181>, under Grant No. FA9550-16-1-0088.

## References

- [1] Offermans P, Schaafsma MC, Rodriguez SRK, et al. Universal scaling of the figure of merit of plasmonic sensors. *ACS Nano* 2011;5:5151–7.
- [2] Baryshnikova KV, Petrov MI, Babicheva VE, Belov PA. Plasmonic and silicon spherical nanoparticle antireflective coatings. *Sci Rep* 2016;6:22136.
- [3] Zhukovsky SV, Babicheva VE, Uskov AV, Protsenko IE, Lavrinenko AV. Enhanced electron photoemission by collective lattice resonances in plasmonic nanoparticle-array photodetectors and solar cells. *Plasmonics* 2014;9:283–9.
- [4] Babicheva VE, Boltasseva A, Lavrinenko AV. Transparent conducting oxides for electro-optical plasmonic modulators. *Nanophotonics* 2015;4:165–85.
- [5] Xiang Y, Dai X, Guo J, Zhang H, Wen S, Tang D. Critical coupling with graphene-based hyperbolic metamaterials. *Sci Rep* 2014;4:5483.

- [6] Staude I, Miroshnichenko AE, Decker M, et al. Tailoring directional scattering through magnetic and electric resonances in subwavelength silicon nanodisks. *ACS Nano* 2013;7:7824–32.
- [7] Cihan AF, Curto AG, Raza S, Kik PG, Brongersma ML. Silicon Mie resonators for highly directional light emission from monolayer  $\text{MoS}_2$ . *Nat Photon* 2018;12:284–90.
- [8] Babicheva VE, Gamage S, Stockman MI, Abate Y. Near-field edge fringes at sharp material boundaries. *Opt Express* 2017;25:23935–44.
- [9] Evlyukhin AB, Reinhardt C, Chichkov BN. Multipole light scattering by nonspherical nanoparticles in the discrete dipole approximation. *Phys Rev B* 2011;84:235429.
- [10] Terekhov PD, Baryshnikova KV, Artemyev YA, Karabchevsky A, Shalin AS, Evlyukhin AB. Multipolar response of nonspherical silicon nanoparticles in the visible and near-infrared spectral ranges. *Phys Rev B* 2017;96:035443.
- [11] Evlyukhin AB, Reinhardt C, Seidel A, Luk'yanchuk BS, Chichkov BN. Optical response features of Si-nanoparticle arrays. *Phys Rev B* 2010;82:045404.
- [12] Babicheva VE. Directional scattering by the hyperbolic-medium antennas and silicon particles. *MRS Adv* 2018;3:1913–7.
- [13] Evlyukhin AB, Novikov SM, Zywiets U, et al. Demonstration of magnetic dipole resonances of dielectric nanospheres in the visible region. *Nano Lett* 2012;12:3749–55.
- [14] Kuznetsov AI, Miroshnichenko AE, Fu YH, Zhang JB, Luk'yanchuk B. Magnetic light. *Sci Rep* 2012;2:492.
- [15] Smirnova D, Kivshar YS. Multipolar nonlinear nanophotonics. *Optica* 2016;3:1241–55.
- [16] Carletti L, Locatelli A, Neshev D, Angelis CD. Shaping the radiation pattern of second-harmonic generation from AlGaAs dielectric nanoantennas. *ACS Photon* 2016;3:1500–7.
- [17] Liu S, Sinclair MB, Saravi S, et al. Resonantly enhanced second-harmonic generation using III–V semiconductor all-dielectric metasurfaces. *Nano Lett* 2016;16:5426–32.
- [18] Lv TT, Li YX, Ma HF, et al. Hybrid metamaterial switching for manipulating chirality based on  $\text{VO}_2$  phase transition. *Sci Rep* 2016;6:23186.
- [19] Babicheva VE, Zhukovsky SV, Lavrinenko AV. Bismuth ferrite as low-loss switchable material for plasmonic waveguide modulator. *Opt Express* 2014;22:28890–7.
- [20] Shcherbakov MR, Vabishchevich PP, Shorokhov AS, et al. Ultrafast all-optical switching with magnetic resonances in nonlinear dielectric nanostructures. *Nano Lett* 2015;15:6985–90.
- [21] Makarov S, Kudryashov S, Mukhin I, et al. Tuning of magnetic optical response in a dielectric nanoparticle by ultrafast photoexcitation of dense electron-hole plasma. *Nano Lett* 2015;15:6187–92.
- [22] Kerker M, Wang DS, Giles CL. Electromagnetic scattering by magnetic spheres. *J Opt Soc Am* 1983;73:765–67.
- [23] Rolly B, Stout B, Bonod N. Boosting the directivity of optical antennas with magnetic and electric dipolar resonant particles. *Opt Express* 2012;20:20376.
- [24] Fu YH, Kuznetsov AI, Miroshnichenko AE, Yu YF, Luk'yanchuk B. Directional visible light scattering by silicon nanoparticles. *Nat Commun* 2013;4:1527.
- [25] Babicheva V, Petrov M, Baryshnikova K, Belov P. Reflection compensation mediated by electric and magnetic resonances of all-dielectric metasurfaces [Invited]. *J Opt Soc Am B* 2017;34:D18–28.
- [26] van de Groep J, Polman A. Designing dielectric resonators on substrates: combining magnetic and electric resonances. *Opt Express* 2013;21:26285–302.
- [27] Zou S, Janel N, Schatz GC. Silver nanoparticle array structures that produce remarkably narrow plasmon lineshapes. *J Chem Phys* 2004;120:10871.
- [28] Markel VA. Divergence of dipole sums and the nature of non-Lorentzian exponentially narrow resonances in one-dimensional periodic arrays of nanospheres. *J Phys B: Atom Mol Opt Phys* 2005;38:L115–21.
- [29] Kravets VG, Schedin F, Grigorenko AN. Extremely narrow plasmon resonances based on diffraction coupling of localized plasmons in arrays of metallic nanoparticles. *Phys Rev Lett* 2008;101:087403.
- [30] Augu   B, Barnes WL. Collective resonances in gold nanoparticle arrays. *Phys Rev Lett* 2008;101:143902.
- [31] Evlyukhin AB, Reinhardt C, Zywiets U, Chichkov B. Collective resonances in metal nanoparticle arrays with dipole-quadrupole interactions. *Phys Rev B* 2012;85:245411.
- [32] Zhou W, Dridi M, Suh JY, et al. Lasing action in strongly coupled plasmonic nanocavity arrays. *Nat Nanotech* 2013;8:506–11.
- [33] Babicheva VE, Evlyukhin AB. Resonant lattice Kerker effect in metasurfaces with electric and magnetic optical responses. *Laser Photonics Rev* 2017;11:1700132.
- [34] Babicheva VE, Evlyukhin AB. Metasurfaces with electric quadrupole and magnetic dipole resonant coupling. *ACS Photon* 2018;5:2022–33.
- [35] Wang W, Ramezani M, V  kev  inen AI, T  rm   P, G  mez Rivas J, Odom TW. The rich photonic world of plasmonic nanoparticle arrays. *Mater Today* 2018;21:303–34.
- [36] Babicheva VE, Evlyukhin AB. Interplay and coupling of electric and magnetic multipole resonances in plasmonic nanoparticle lattices. *MRS Commun* 2018. doi: 10.1557/mrc.2018.112.
- [37] Arslan D, Chong KE, Miroshnichenko AE, et al. Staude: Angle-selective all-dielectric Huygens' metasurfaces. *J Phys D Appl Phys* 2017;50:434002.
- [38] Yang Ch-Y, Yang J-H, Yang Z-Y, et al. Nonradiating silicon nanoantenna metasurfaces as narrowband absorbers. *ACS Photon* 2018;5:2596–601.
- [39] Decker M, Staude I, Falkner M, et al. High-efficiency dielectric Huygens' surfaces. *Adv Opt Mater* 2015;3:813–20.